



Comparison of the fluctuations of the signals measured by ICP-MS after laser ablation of powdered geological materials prepared by four methods

Michaël Susset¹ · Axelle Leduc--Gauthier¹ · Anne-Claire Humbert¹ · Fabien Pointurier¹ · Christophe Pécheyran²

Received: 25 December 2022 / Accepted: 17 February 2023 / Published online: 1 March 2023
© The Author(s), under exclusive licence to The Japan Society for Analytical Chemistry 2023

Abstract

Sample preparation is a crucial point for quantitative multi-elemental analyses by LA-ICP-MS of powdered geological materials. Four different methods are compared in this study with respect to signal stability and intensity as follows: the preparation of glass beads (GlassB) by alkaline fusion method and three grinding and pelletizing methods relying on the use of an organic binder (VanBind, vanillic acid), an adhesive binder (MixGlue, methyl methacrylate) and a sol–gel process for glass formation (SolGel, chemical reaction of tetraethoxysilane), respectively. Sixty elements were analyzed by means of a ns-UV (213 nm) laser ablation system coupled to a single collector sector field ICP-MS with a low or medium mass resolution. Signal stability was found to strongly depend on the sample homogeneity provided by the preparation method. These methods were applied to three geological standard materials (CRM). The following criteria were used to evaluate and compare the methods: (1) proportion of the measurement cycles which are above a given signal intensity threshold (defined here as signal average ± 3 times the standard deviation), (2) signal stability of the analyzed nuclides (internal precision estimated by the relative standard deviations on raw count rates), (3) signal stability of the internal standards added to the samples, (4) external precision estimated by the relative standard deviation over five preparations for each geological CRM. For the majority of the analyzed elements, signals measured for samples prepared with the four methods are reproducible. Specific contamination in one or several elements (Cr, Fe, Co, Ni, Cu, Mo, W, Au and Bi) was observed depending on the sample preparation method. In addition, compared to grinding made with PTFE material, grinding performed with tungsten carbide material was found to produce better homogeneity, especially for the sol–gel and mixing with glue protocols, although some metallic contamination (W and Co) was observed. Thanks to the suppression of grain effects by alkaline melting, the glass bead method systematically provided signal stability and percentage of “over the threshold” close to those of the NIST glasses. This may be explained by the preparation of more homogeneous samples by alkaline melting. Finally, the described methods were found to be reproducible for the majority of the analyzed elements.

Keywords LA-ICP-MS · Sample preparation · Homogeneity of the samples · Geological samples · Glass bead · Pellet

Introduction

The coupling between a laser ablation device and ICP systems has been implemented many times for specific applications such as the analysis of geological samples [1–15],

the analysis of elemental impurities for the nuclear industry [16–18], archaeological studies [19, 20], etc.

For measurement of elemental composition of heterogeneous samples, the shaping of powdered materials before analysis by LA-ICP-MS is essential to avoid dust particle dissemination into the laboratory and to homogenize the samples. In the specific case of the analysis of nuclear materials, it is of uttermost importance to avoid losing particles within the ablation cell or in the facility. Various methods have been described in the literature: formation of glass beads by alkaline fusion [1–3, 21], pelletizing with an organic binder [9, 17, 22–25], glass formation by sol–gel

✉ Michaël Susset
michael.susset@outlook.fr

¹ CEA, DAM, DIF, 91297 Arpajon, France

² Université de Pau et des Pays de l'Adour, E2S UPPA, CNRS, IPREM, Avenue de l'Université, 64012 PAU Cedex, France

process [26–28], mixing with an adhesive compound [29], nano-particulate pressed powder tablets [30, 31], deposition on an adhesive surface [32], sintering [33], formation of a zinc complex [34], pelletizing after NH_4HF_2 digestion [35].

Many authors use the fluctuations of the LA-ICP-MS signals to estimate the homogeneity of the aerosol and consider that homogeneity of the LA aerosol is related to the homogeneity of the sample [1, 3, 6, 8, 12, 22, 24, 28, 29, 36–40]. Baker et al. [5] reported that the sudden increases in signal intensities they observed (referred to as “spikes”) may be due to heterogeneities in the sample. The theoretical advantage of using LA-ICP-MS to evaluate sample homogeneity is to provide potentially both information on the homogeneity of the aerosol and elemental composition of the sample. The fluctuations’ sources of the signal are depending on laser ablation parameters and sensitivity of the spectrometer, so the signal fluctuations reported in the literature could not be compared easily between articles. Very few studies deal with the comparison of different sample preparation methods.

Jantzi et al. [32] compared tape mounting (deposition onto an adhesive tape) versus pelletizing for LIBS and LA-ICP-MS analysis and concluded that the tape mounting method gives similar or lower relative standard deviations (RSD) of the signals than the pellets (non-milled soil samples).

Wu et al. compared ultrafine pellets versus flux-free fusion glasses [36] and concluded that the homogeneity of fusion glass (50 μm spot size) is better than the ultrafine powder pellets (90 μm spot size).

Jochum et al. [31] demonstrated that the reproducibility of measurements obtained with nano-particulate pressed powder pellets was lower by a factor 2–3 compared to “original powder pellets”.

O’Connor et al. [24] compared different kinds of pellets as follows: with vanillic acid [i.e., poly(vinyl alcohol)] as binder or without binder. The use of the vanillic acid allowed obtaining more stable signals compared to the others discussed methods. In addition, compared to nicotinic acid and pyrazinoic acid, other chromophore binders, the use of the vanillic acid resulted in an increase of the sensitivity.

Peters and Pettke [41] compared the following seven binders: polyvinyl alcohol, nicotinic acid, pyrazinoic acid, graphite, collagen hydrolyzate, microcrystalline cellulose and vanillic acid. These last two binders produced the most mechanically stable pellets, whose analysis by LA-ICP-MS produced the smallest measurements uncertainties and the best measurement repeatability.

Our final objective was to carry out quantitative elemental analysis by means of LA-ICP-MS. To achieve this goal, signals must be as stable as possible and the very small mass of material sampled by laser ablation (typically in the ng to μg

range) must be representative of the original material, which implies that the sample submitted for analysis is sufficiently homogenous. Moreover, the chosen method must allow the addition of one or several internal standards homogeneously distributed in the sample in order to correct for variations in the sensitivity of the LA-ICP-MS signals. These signal variations originated from all the analytical steps, i.e., laser sampling, aerosol transport, particle atomization in the ICP, ionization and ion extraction, focusing and detection. Moreover, the sample preparation must be reproducible and thus lead to similar sensitivity and stability between different samples prepared from the same material.

In this article, four preparation methods were applied to three powdered geological certified reference materials (CRM), certified for concentrations of several chemical elements of various abundances (from ng/g to percent). These four methods are as follows: (1) mixing with a glue (Mix-Glue), (2) mixing with an organic binder (VanBind), (3) glass formation by sol–gel process (SolGel) and (4) glass beads’ (GlassB) formation by alkaline melting. For the first three methods, the samples must be grinded and pelletized. Grinding were carried out either with PTFE material or tungsten carbide (WC) material.

The aims of this work are to compare the preparation methods according to the four following criteria: (1) the number of measurement cycles for which sharp increases in intensity above a given threshold are detected, (2) internal precision of the raw signals for the 58 nuclides of interest, (3) the internal precision of the raw signals for the two internal standards added to the materials, and (4) the external precision of the sample for the 60 measured nuclides (reproducibility of the preparation protocols).

To our knowledge, this is the first time that a comprehensive comparison of as much sample preparation methods of powdered materials for multi-elemental LA-ICP-MS analysis is reported. Indeed, previous publications on the same topic turned on comparisons between at most two preparation methods.

Material and methods

Instrumentation

Analyses were performed with an Element XR ICP-MS (Thermo Fischer Scientific, Bremen, Germany). The instrument configuration is a double-focusing Nier-Johnson geometry sector field. The instrument is equipped with the so-called jet interface, which consists of a high-performance interface pump, a Ni ‘H’ skimmer cone and a Ni sampler cone. Settings are described in Table 1. The introduction system consists of a cyclonic spray chamber, a micro-nebulizer (PFA, 100 $\mu\text{L}/\text{min}$) operated in self-aspiration mode to nebulize a 2% HNO_3 solution.

Table 1 Settings of the ICP-MS and the ablation laser system

ICP-MS settings		Laser ablation settings	
Nebulizer	PFA, 100 μ L/min	Ablation cell	HelEx
Nebulization chamber	Cyclonic glass expansion spray chamber	Wavelength	213 nm
Cool gas (Ar)	16 L/min	Gas (He)	0.8 L/min
Auxiliary gas (Ar)	\approx 0.75 L/min	Spot diameter	100 μ m
Sample gas (Ar)	\approx 0.70 L/min	Scan speed	10 μ m/s
Cones	Ni 'H' skimmer cone Ni sampler cone	Frequency	20 Hz
		Fluence	15, 14, 13 and 11 J/cm ² *

*For the glass bead, the mixing with glue method, the mixing with vanillic acid method and the sol-gel process, respectively

A Teledyne CETAC (Omaha NE, United States) LSX-213-G2+ nanosecond laser ablation system operating at 213 nm was used. The instrumental parameters were optimized to minimize both the signal fluctuation and the elemental fractionation (U/Th ratio) and to increase the signal intensity. Analytical parameters are reported in Table 1. Fluences of 15 J/cm², 14 J/cm², 13 J/cm², and 11 J/cm² were applied to the glass beads, the mixing with glue, the sol-gel technique and the mixing with an organic binder, respectively. The ablations were performed as straight lines.

Solid and liquid aerosols were mixed just before their injection in the ICP-MS system thanks to a T-shape glass connection piece.

All the grindings described in the sample preparation part were carried out with a MM400 mill (Retsch, The Netherlands). The press used is an Atlas manual 15 T hydraulic press (Specac, Orpington, United Kingdom).

Certified reference materials

Three CRM of different geological origins and matrices available in the laboratory, referred to as "geostandards", were analyzed: (1) GS-N, a granite (Centre de Recherches Pétrographiques et Géochimiques, CNRS, France), (2) NCS DC73301, an undefined mineral (China National Analysis Center for Iron and Steel, China), (3) ZW-C, a zinnwaldite (Centre de Recherches Pétrographiques et Géochimiques, CNRS, France). These materials were chosen because their concentrations in many elements were certified.

The NIST 612 and 614 glasses (National Institute of Standards & Technology, USA) CRMs were also analyzed [42, 43].

Acquisition parameters and ablation scheme

LA-ICP-MS signals corresponding to 56 elements of interest for the laboratory were measured. For some of these elements, signals of two nuclides were recorded; a total of 61 nuclides were measured.

Signals of the following 40 nuclides (corresponding to 37 different elements) were acquired in the low-resolution (LR) mode ($R=300$): ⁹Be, ⁸⁸Sr, ⁸⁹Y, ⁹⁰Zr, ⁹³Nb, ^{95,97}Mo, ¹⁰³Rh, ¹⁰⁷Ag, ¹¹¹Cd, ¹¹⁵In, ¹¹⁸Sn, ¹²¹Sb, ¹²⁵Te, ^{137,138}Ba, ¹³⁹La, ¹⁴⁰Ce, ¹⁴¹Pr, ¹⁴⁶Nd, ¹⁴⁷Sm, ¹⁵³Eu, ¹⁵⁷Gd, ¹⁵⁹Tb, ¹⁶³Dy, ¹⁶⁵Ho, ¹⁶⁶Er, ¹⁶⁹Tm, ¹⁷²Yb, ¹⁷⁵Lu, ¹⁷⁸Hf, ¹⁸¹Ta, ¹⁸²W, ¹⁹⁷Au, ²⁰⁵Tl, ^{206,208}Pb, ²⁰⁹Bi, ²³²Th and ²³⁸U. Signals of 21 nuclides (corresponding to 19 elements) were measured in the medium resolution (MR) mode ($R=4000$) in order to remove potential polyatomic interferences: ²⁴Mg, ²⁷Al, ⁴⁴Ca, ⁴⁵Sc, ⁴⁷Ti, ⁵¹V, ^{52,53}Cr, ⁵⁵Mn, ^{56,57}Fe, ⁵⁹Co, ⁶⁰Ni, ⁶³Cu, ⁶⁶Zn, ⁶⁹Ga, ⁷²Ge, ⁷⁵As, ⁷⁷Se, ¹⁰³Rh and ¹¹⁵In.

Short dwell times were chosen to capture the signal variability. It should be mentioned that the hysteresis of the magnetic field significantly increases the total duration of the measurement when it is highly fractionated in a large number of cycles with short dwell times (poorer useful duty cycle). The total analysis time for an ablation line is 7.7 min, including 150 measurements of 15 ms per nuclide in the LR mode (peak defined by three points) and 45 measurements of 360 ms per nuclide in the MR mode. However, in the MR mode, the real measurement time is 30 ms as only 10% of the peak width (the three points the closest to the peak center) are considered. The three geostandard samples prepared according to the four methods described below were then ablated according to lines of 0.46 mm² (4.6 mm \times 0.1 mm) in triplicate.

As described before, RSD will depend on the acquisition parameters; for this study, short analysis times have been selected to have a fast sampling of the signal despite an enhancement of the RSD measured.

In addition, to provide a visual examination of the signal fluctuations, 2D mappings were carried out using an in-house method in LR mode for the following nuclides: ⁴⁷Ti, ⁵¹V, ⁵³Cr, ⁵⁷Fe, ⁵⁹Co, ⁶⁰Ni, ⁶³Cu, ⁶⁶Zn, ⁸⁸Sr, ⁸⁹Y, ⁹⁰Zr, ⁹⁵Mo, ¹⁰³Rh, ¹¹¹Cd, ¹¹⁵In, ¹³⁸Ba, ¹³⁹La, ¹⁴⁰Ce, ¹⁴¹Pr, ¹⁴⁶Nd, ¹⁴⁷Sm, ¹⁵³Eu, ¹⁵⁷Gd, ¹⁵⁹Tb, ¹⁶³Dy, ¹⁶⁵Ho, ¹⁶⁶Er, ¹⁶⁹Tm, ¹⁷²Yb, ¹⁷⁵Lu, ¹⁸²W, ²⁰⁶Pb, ²³²Th and ²³⁸U. The scan speed of the laser has been adapted (19.2 μ m/s) together with the line spacing and signal acquisition speed to have one measurement of each nuclide every 20 μ m (square pixels) on a total 1.75 mm \times 3.5 mm surface.

Preparation methods

Four methods previously described in the literature and suitable for the preparation of powdery samples were selected.

These methods should allow synthesis of sufficiently homogeneous, mechanically robust samples, should be stable for long-term storage and easy to implement in the laboratory. In addition, they should allow the introduction of internal standards and require only commonly available laboratory reagents and equipment, including binders or other compounds.

Grinding steps

Three of the four preparation methods (MixGlue, VanBind and SolGel, see below) required a mixing and grinding step followed by pelletizing.

Two following materials were used for the milling balls:

- Teflon coated balls with an iron core and PTFE bowl: despite a lower milling efficiency, they were chosen because PTFE does not lead to contamination in elements of interest (Cr, Zr, Si, Co, Fe, etc.), contrary to metallic balls and bowls. Mixing-grinding conditions were: 10 min at 30 Hz in a 25 mL PTFE bowl with a 10 mm diameter iron core coated by Teflon.
- Tungsten Carbide (WC) was selected to ensure a more efficient grinding. Mixing-grinding conditions were: 10 min at 30 Hz in a 10 mL WC bowl with 20 WC balls of 5 mm diameter.

It should be mentioned that longer milling process, either with PTFE or WC balls, did not significantly decrease the size distribution. The pelletizing step was strictly identical for the MixGlue and SolGel methods, i.e., 120 mg of each mixture was pelletized under 4 tons of pressure for 3 min to form pellets of 6 mm diameter (side opening mold, Euro Labo). In the case of the VanBind preparation method, 120 mg of the obtained powder was pressed under 2 tons for 3 min to form a 5 mm-diameter pellet (evacuable pellet dies, Specac).

Method 1: preparation with mixed glue (MixGlue)

Klemm and Bombach [29] reported a simple preparation which consists in mixing the powdered sample with a glue (methyl methacrylate). The same glue as Klemm and Bombach was used. However, the method of Klemm and Bombach was slightly modified (addition of a small amount of ammonium nitrate, drying in an oven before pelletizing). 2 mL of methyl methacrylate (99% purity, Acros Organics) in 18 mL of acetone was mixed with 129 μL of In (with 2% of HNO_3) and Rh (with 5% of HCl) at about 1 g/L. 500 mg of sample were mixed with 50 mg of ammonium nitrate (99% purity, Merck). These two compounds were mixed using the lateral mechanical agitation provided by the mill without balls. Mechanical stability of the sample was ensured by

oxidization through the addition of ammonium nitrate. 1 mL of the diluted methyl methacrylate solution was added to this powder and the whole was stirred for 1 hour with the grinder without grinding balls. The mixture was then placed in an oven at 95 °C overnight. The dry agglomerated powder recovered was then mixed, ground and pelletized as previously described.

Method 2: preparation by compression into pellets with an organic binder (VanBind)

Vanillic acid was previously used by O'Connor et al. [24]. Their protocol was slightly modified (addition of Rh and In in liquid form). 120 mg of solid vanillic acid (98% purity, Merck) and 180 mg of geostandard material were mixed. Then, 430 μL of an internal standard solution of In and Rh at 7 mg/L in ultrapure water (18.2 MOhm, Millipore), with 0.035% of HCl and 0.014% of HNO_3 , were added. Note that this solution contained trace amounts of HCl and HNO_3 due to dilution of the stock solutions. The whole was mixed for 10 min at 30 Hz and the mixture was then placed in the oven overnight at 110 °C. The dry powder was then mixed, ground and pelletized as previously described.

Method 3: preparation by means of the sol-gel method (SolGel)

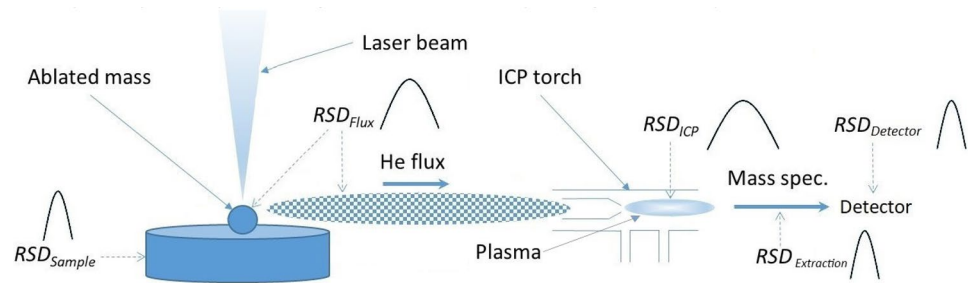
The method implemented in this work is the one described by Hubová et al. [26] for the preparation of agricultural soil samples for analysis by LA-ICP-AES. Again, this protocol was modified (addition of a small amount of ammonium nitrate).

300 mg of sample was weighed into a 2-mL tube with a rounded bottom. 50 mg of ammonium nitrate (99% purity, Merck) was added and mixed to the sample using the mill used without balls at 30 Hz for 1 hour. Meanwhile, the following mixture was prepared: TEOS (99.999 + % purity tetraethoxysilane, $\text{Si}(\text{OC}_2\text{H}_5)_4$, Alfa Aesar), absolute ethanol (VWR), ultrapure water spiked with 10.5 μL of a 1 g/L of In (with 2% of HNO_3) and Rh (with 5% of HCl) in the proportions 3: 6: 2 (v: v: v; 0.75 mL/1.5 mL/0.5 mL). At the end of the mixing, the powder was added to the prepared liquid mixture. The mixture was heated and stirred in a sonication bath at 75 °C for 1.5 h. 1 mL of water was added to the mixture after 20 min of sonication to avoid dehydration. The whole was then placed overnight in the oven at 110 °C. The dry powder was then mixed, ground and pelletized as previously described.

Method 4: preparation of the glass beads (GlassB)

The glass beads were prepared with a Katanax X-Fluxer X-600. The sample and all the chemicals were weighed,

Fig. 1 schematic representation of the different sources of signal fluctuations



mixed and fused at 1055 °C in platinum crucibles (95% Pt and 5% Au).

0.75 g of sample and 0.5 g of ammonium nitrate (98% purity, VWR) were mixed manually and placed in a crucible. Then, 190 μ L of a solution of 0.1 g/L In and Rh, 2 g of lithium metaborate (LiBO_4 , ultrapure quality, SCP Science), 0.5 g of lithium bromide (LiBr, 99% purity, Merck) and 5.5 g of lithium tetraborate ($\text{Li}_2\text{B}_4\text{O}_7$, ultrapure quality, SCP Science) were added.

The crucibles were then introduced into the furnace. The temperature program was as follows: (1) 5 min at 500 °C, (2) increase of the temperature to 1055 °C, (3) pendulum stirring with an inclination of 25° for 10 min, (4) a more intensive stirring with an inclination of 30° for 1 min, (5) removal of the samples from the furnace and immediate transfer into the glass bead cups, (6) 5 min cooling time outside the furnace, and (7) last, 45 s cooling time with a fan.

The glass bead machine allows the production of six glass beads at the time.

Data treatment

For some nuclides, count rates are very low, close to instrumental background. Thus, nuclides for which integrated numbers of counts are lower than 10 counts or lower than three times the average instrumental background (signal recorded only with He gas, without laser ablation) plus 3 times its standard deviation were not considered. The list of these nuclides is given in the Supplementary Information 1.

Signal filtering

Time resolved LA-ICP-MS signals showed high variability for all measured elements. Indeed, signal “spikes” (i.e., very sharp and very brief increase of the signals) were systematically observed during the line ablations for all the measured nuclides. This phenomenon had already been reported by many authors for line-scan LA-ICP-MS analysis of soil or sediment samples [5, 44–46]. No signal spikes are observed during background measurements between samples, so these spikes are not due to memory effects. The measurements whose count rates were too far from the average count rates

were regarded here as outliers and removed. For that, an outlier rejection treatment was implemented. More precisely, a measurement was regarded as an outlier when its count rate is above or below the average count rate ± 2 or 3 times the standard deviations (SD) over all the measurements of an ablation line. The outliers were eliminated using an iterative process that ended when no more outliers were identified.

After the removal of all the outliers, average count rates and associated standard deviations were calculated with the remaining values for each nuclide. In the following, only non-rejected values with a $3 \times \text{SD}$ filter were considered.

Signal normalization

Two internal standards (^{103}Rh and ^{115}In) were added to the materials. In the current study, results obtained with the two internal standards were in very good agreement and only the ones with ^{103}Rh were presented and discussed.

Sources of signal fluctuations

To compare the signal fluctuations, internal RSDs were measured for each nuclide and for each sample. Internal RSDs depend on multiple factors. Laser ablation of a solid material and transmission of ablated particles in the ICP source are very complex phenomena. However, in addition to the statistical counting error, we schematically distinguish here the following factors that affect the signal fluctuations (Fig. 1): (1) variation of the ablation efficiency (i.e., a variation of the ablated mass per laser pulse), (2) variation in the flux of ablated material introduced into the plasma (which depends on the initial-particle size distribution, the fluctuation of their transport efficiency, the laser repetition rate and the homogeneity of the sample), (3) variation in the ICP atomization/ionization efficiency, and (4) variation in the ion extraction efficiency. The d_{10} , d_{50} and d_{90} of the three CRM before the grinding step are between 1.6 and 3.3 μm , 8.2 and 16.1 μm and 40 and 101 μm , respectively, according to measurements by laser granulometry.

Therefore, assuming all these fluctuations are independent, the internal RSD can be written as follows:

$$RSD_{\text{internal}} = f(RSD_{\text{Sample}}, RSD_{\text{Flux}}, RSD_{\text{ICP}}, RSD_{\text{Extraction}}, RSD_{\text{Detector}}),$$

where RSD_{Sample} , RSD_{Flux} , RSD_{ICP} , $RSD_{\text{Extraction}}$, RSD_{Detector} are the RSD caused by variations in sample surface homogeneity, ablation efficiency, particle flux, atomization/ionization efficiency, ion extraction and statistical error of the detection, respectively.

We consider here that RSD_{Flux} and RSD_{Sample} are the major source of fluctuations. Indeed, variations of the signal intensities due to the ICP energy fluctuation are expected to be relatively small with respect to the duration of the measurement of a single sample (7.7 min).

Internal precision (repeatability) and external precision (reproducibility)

For each measured nuclide, three types of RSDs were considered in order to compare the performance of the preparation methods as follows: two “internal” RSDs for the intra-preparation’s fluctuation at different analyzed scales, namely RSD(int small) and RSD(int large), and one “external” RSD for the inter-preparation’s fluctuation, RSD(ext).

These two internal RSDs were calculated from data points corresponding to two spatial resolutions. The first, RSD(int small), corresponds to the surface ablated during a single acquisition point at the laser stage speed of 10 $\mu\text{m/s}$ and a laser beam diameter of 100 μm . Taking into account the number of isotopes and acquisition parameters described above, this corresponds to approximately 0.0019 mm^2 in the LR mode and 0.0037 mm^2 in the MR mode. 150 points were then considered in LR and 45 points in MR. The second internal RSD, hereafter referred to as RSD(int large), was calculated from 5 measurement points, each corresponding to a large ablated area of approximately 0.0380 mm^2 in LR and 0.0338 mm^2 in MR. According to Neuilly, estimation of the SD is unbiased only if the number of data points is sufficiently large, in practice larger or equal to 5 [47].

“External” RSD, called RSD(ext), was calculated from five samples from the GS-N standard prepared independently by each preparation method described below. Ablated areas were estimated to be 0.29 mm^2 in LR and 0.17 mm^2 in MR.

RSD(ext) and RSD(int large) were calculated after signal normalization with the internal standard. No normalization was made for calculation of the RSD(int small), because significant increases of the RSD(int small) were observed after signal normalization. Indeed, we think that the internal standardization allows correcting efficiently the “long-term” signal variation of the instrument’s sensitivity, but not the “short-term” variations of the signal intensities evaluated by the RSD(int small). This might be due to the short-term variations of signals of the nuclides of interest and of the internal standards captured by the RSD(int small) are dominated

by local heterogeneities in the samples and variations in the sampling LA process, rather than by variations of the instrumental sensitivity.

Comparison of the internal precision with the counting statistic error

If only random statistical errors are involved, theoretical RSD is given on average by the Poisson distribution as follows:

$$RSD_{\text{Poisson}} = \frac{1}{\sqrt{n}} \times 100,$$

where n is the average number of counts of the data points considered for the RSD calculation.

This comparison between the internal RSD and Poisson’s RSD can also be expressed mathematically by the Fano factor, which was described for the first time in 1947 [48, 49]. It represents the dispersion of a probability of Fano noise. The Fano factor, F_X of the nuclide X , is calculated as follows:

$$F_X = \frac{\sigma_{I_X}^2}{I_X} = \frac{\sigma_{I_X}^2}{\sigma_{\text{Poisson}}^2} = \frac{RSD_{I_X}^2}{RSD_{\text{Poisson}}^2},$$

where I_X is the average of the three signal intensities and σ_{I_X} is the average of the standard deviations of the signals. For a Poisson process F_X equal to 1, the single source of error is the statistical error on counting by the detection system. If the internal RSDs are systematically higher than the Poisson’s RSDs (i.e., $F_X > 1$), then other source of errors than random counting are predominant. On the contrary, if the internal RSDs and the Poisson’s RSDs are on average reasonably close (i.e., F_X close to 1), then the random counting error is the major source of error. In other words, the Fano factor is an interesting tool to determine the relative importance of random counting error and of other sources of errors. Therefore, in the current study, RSD(int small) will be systematically compared to the Poisson’s RSDs.

Results and discussion

Internal precision (repeatability) of the measurements

Comparison of the proportion of filtered values

The proportion of measurement cycles rejected by the $\pm 3 \times \text{SD}$ filter described above is an indicator of the signal stability. In a first step, in order to compare the proportion of rejected measurements and see their spatial distribution according to the preparation modes, a 2D mapping of a few nuclides was carried out for the four preparation

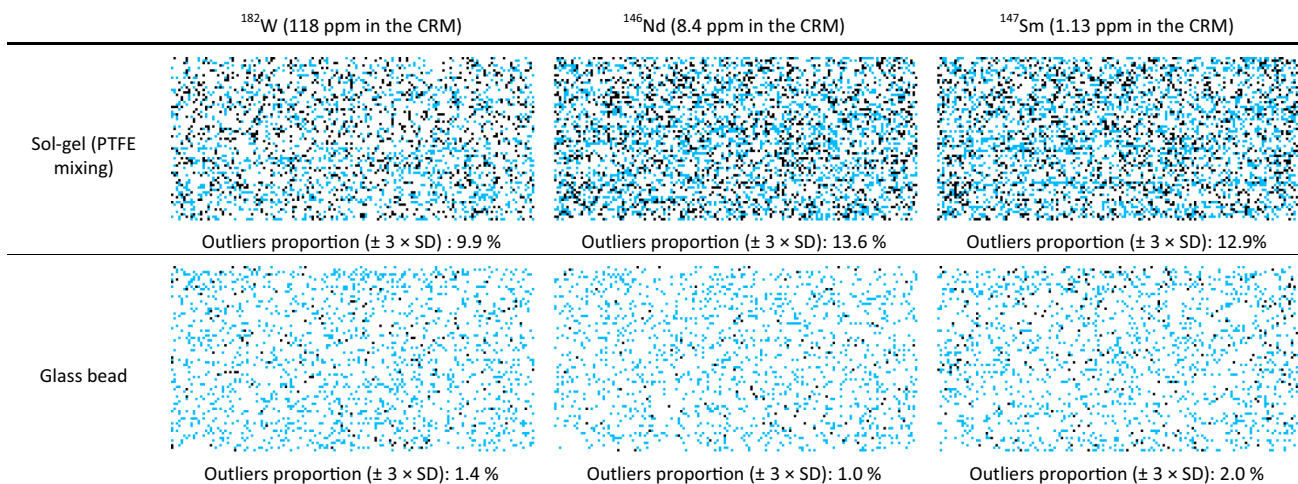


Fig. 2 typical example of LA-ICP-MS imaging of the GS-N standard (1.75 mm × 3.5 mm) with a 20 μm resolution. Over-ranged values at ± 3 × SD (black points) and ± 2 × SD (blue points) are presented for

two different preparation methods and for three nuclides with different concentrations

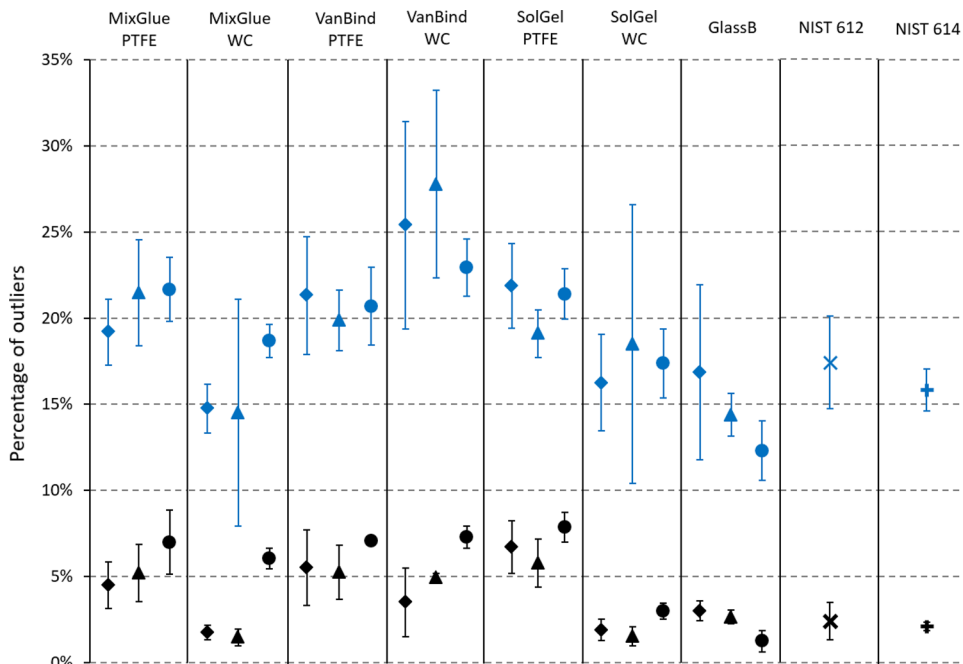
methods (milling with PTFE only for the pelletizing methods). For this, the GS-N geological material was ablated. 2D images are given as examples for the GlassB and the SolGel/PTFE methods in Fig. 2. The other images are given in the Supplementary Information 2. In addition, the averages' percentage of removed measurement cycles (also ± 3 × SD filtering) are plotted for all preparation methods and geological materials (Fig. 3).

As shown in the examples presented in Fig. 2, signal spikes observed for all nuclides were randomly distributed. They are not gathered in “clusters” of an excess of

intensities, which would have indicated the presence of grains larger than the ablated surface which corresponds to a measurement. Therefore, formation of the spikes is the consequence of random variations in ablation efficiency and particle transport and/or to heterogeneities smaller than the surface ablated during a measurement. In other respects, no apparent correlation was observed from these images between the signal intensity and the proportion of rejected values (Fig. 2 and Supplementary Information 3).

The percentages of outliers for each sample and preparation method are compared in Fig. 3. Here, the values

Fig. 3 comparison of the proportions of ± 2 × SD (blue points) and ± 3 × SD rejected values (black points) for the four preparation methods (PTFE and WC refer to the use of PTFE and WC balls during mixing/ grinding process, respectively) applied to the three CRM studied (3 ablation lines). Diamonds are for GS-N, triangles for NCS DC73301 and circles for ZW-C. Rejected values on NIST glass CRM (9 lines) are also reported



correspond to ablated areas of 0.0019 and 0.0037 mm² in LR and MR modes, respectively.

The proportions of $\pm 2 \times SD$ and $\pm 3 \times SD$ rejected values are high, well beyond the expectations of a Gaussian distribution ($\sim 2\%$ and $\sim 0.15\%$ of values higher than $\pm 2 \times SD$ and $\pm 3 \times SD$, respectively). This is consistent with high variability of the time-resolved signals. Even in the case of NIST glasses that can be regarded as homogeneous materials, percentages of $\pm 2 \times SD$ and $\pm 3 \times SD$ outliers are very high, in the range of 15–20% and 1.5–3.5%, respectively. It should be mentioned that these values depend on the acquisition parameters. Indeed, increasing the acquisition time will certainly smoothen the signals. However, information related to “short-term” variations, including the proportion of filtered values, will be lost.

A measurement rejected by the $\pm 3 \times SD$ filtering may be the consequence of a local heterogeneity of concentration, a higher density of ablation particles arriving in the plasma or ablation particles larger than a “critical size”, above which the particles are not fully analyzed by the ICP-MS (incomplete atomization and ionization). Figure 3 shows clearly that fewer outliers are observed for the GlassB and NIST glasses with respect to pellets with PTFE grinding. Percentages of outliers for GlassB are similar to the ones of NIST glasses 612 and 614. These results may be explained by the suppression of grain effects by the alkaline fusion method, whatever the material is and/or by production of smaller ablation particles. Grinding with WC balls slightly reduces the percentage of outliers compared to grinding with PTFE balls when using a $\pm 3 \times SD$ filter, at least for SolGel and MixGlue. The decrease in the percentage of $\pm 2 \times SD$ outliers allowed by WC grinding is also observed but to a lesser extent than with the $\pm 3 \times SD$ filtering. It is expected that the use of a harder milling material produces a smaller granulometry of the sample. In addition, the number of balls and the volume of the bowl (which are different between the grinding with the PTFE and the WC materials) also have an influence on the efficiency of the grinding. Therefore, acquisition of more stable signals with the grinding carried out with the WC material is not only due to the higher hardness of the material used but also to the more favorable grinding conditions (i.e. more balls and a smaller bowl). In the following, only the material nature will be mentioned, although it is understood that the grinding conditions have a strong influence. Interestingly, percentages of outliers when WC grinding was applied to SolGel and MixGlue are comparable, and even lower in some cases, than the percentages of outliers for glassy samples (NIST glasses and GlassB). However, surprisingly, grinding with WC balls does not lower the percentage of outliers in the case of VanBind, for all the three geostandards. We assume that both grinding with PTFE and WC balls leads to heterogeneities by agglomeration of vanillic acid.

Evaluation of the internal precision using RSD(int small)

The RSD(int small) are plotted against the signal intensity in Fig. 4 for the GS-N CRM. The same graphs are given in Supplementary Information 4 for NCS DC73301 and ZW-C. RSD(int small) for NIST glasses 612 and 614 are also plotted for comparison. Observations were similar for the three CRM.

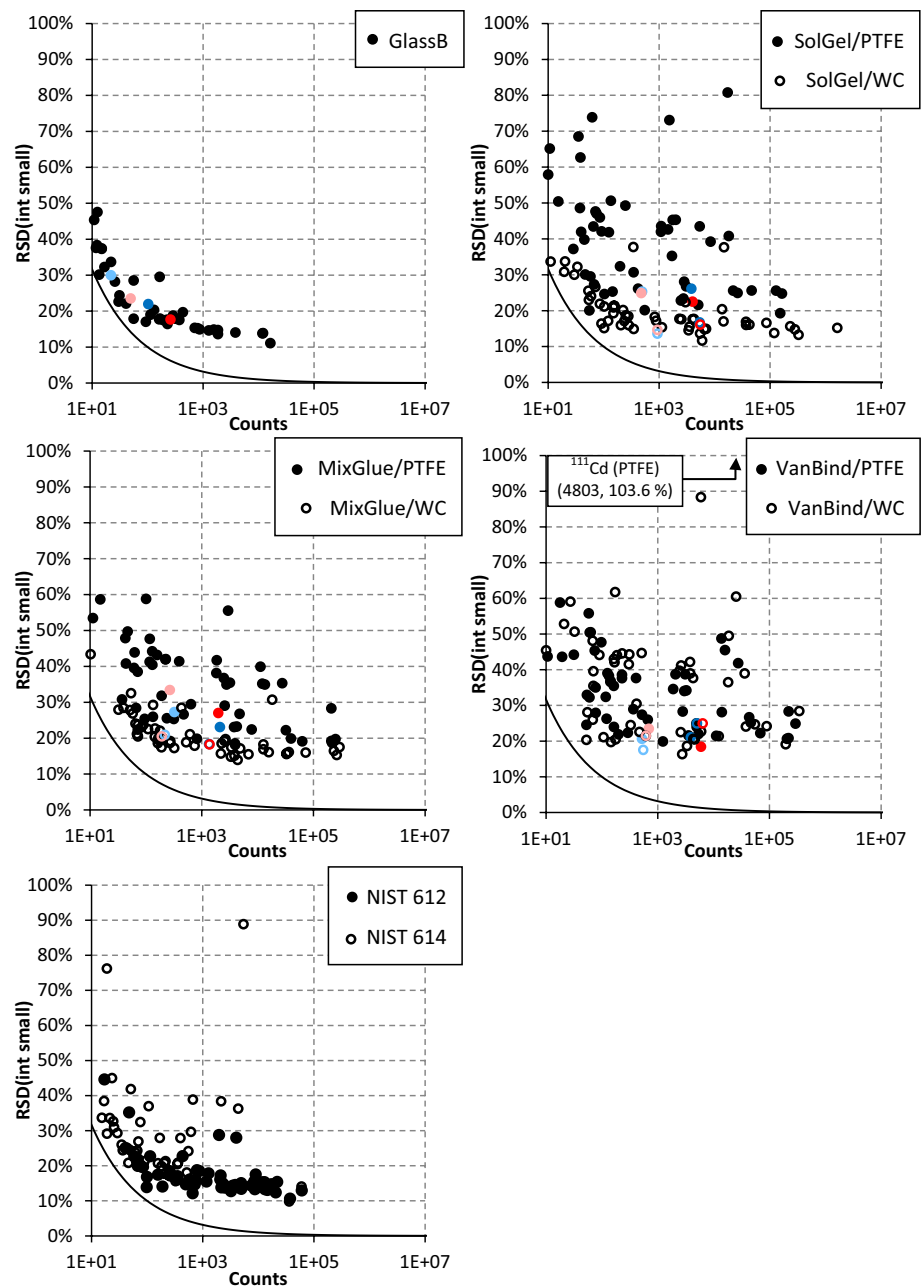
For all of the three samples, RSD(int small) of GlassB are similar to those obtained with NIST glasses (in the range 10–15% for most nuclides with a number of counts higher than 10^3 within the conditions of these experiments). Note that RSD for the perfectly transparent NIST 614 are higher than with NIST 612 as larger particles are produced when ablating transparent glasses [50].

The RSD(int small) for MixGlue and SolGel are lower when grinding is carried out with WC beads than with PTFE, typically in the 15–20% range for count rates higher than 10^3 with WC grinding instead of 20–40% with PTFE grinding. In contrast, grinding with WC does not improve precision in the case of VanBind (most RSD(int small) are in the 20–50% range for both grinding materials). These observations are consistent with those described in the previous section. For all of the materials, the lowest RSDs(int small) are obtained for GlassB, which indicates that the ion flux arriving at the detector is more stable than for the methods that require a pelletizing step. This is certainly due to the suppression of the grain effects. However, the improvement in precision with respect to other methods is reduced when the grinding is performed with WC balls.

As shown in Fig. 4, RSDs(int small) are systematically higher than RSD(Poisson) for the same number of counts, which indicates that counting statistics is not the major source of error at least for average numbers of counts per measurement cycle higher than $\approx 10^3$. Besides, it seems that the RSDs(int small) reach a plateau for all preparation methods. The values of the plateau, estimated by the average of RSD(int small) of all the signals higher than 10^3 counts, are 14% for GlassB (likewise NIST 612 glass, 16%) and 18% for SolGel and 21% for MixGlue with WC grinding, within the conditions of these experiments. Values of the plateau are more difficult to define for the other methods (VanBind and all methods grinding with PTFE), owing to the wide dispersion of the RSD(int small). This plateau phenomenon is caused by errors that are not linked to counting statistics, i.e., variations in the particles transport, in the ablation efficiency, in the atomization/ionization and in ion extraction efficiency.

As detailed before, these RSD values are higher than the ones reported in the literature, which in reality are relative deviation of the mean or RSE (RSD divided by the square root of the number of measurements). Here, calculated RSE are generally lower than 4% (for signals higher than 10^3

Fig. 4 averaged RSD(int small) ($n=3$) as a function of count rates obtained on the GS-N geostandard material analyzed with the four preparation methods carried out in this study. Values obtained for NIST series glass are also reported. RSD(int small) was calculated from 150 measurements in LR and 45 measurements in MR for all measurements. Each point corresponds to one nuclide. The black curves represent the RSD calculated according to the Poisson's distribution. The red symbols are for In and the blue symbols for Rh. The symbols in light colors are for the MR mode and the symbols in dark color are for the LR mode



counts) for all the sample preparation methods, and even lower than 2% for the GlassB method.

The difference between counting statistics errors and the variability of signals resulting from the heterogeneity of preparations or the LA sampling process can also be evaluated thanks to the Fano factor. Statistical data (average, median value, etc.) about Fano factors are given in the Table 2. Fe and Cr were discarded for the pelletizing methods (press components), W and Co when WC material was used, and elements which have a concentration found as non-reproducible were discarded (see next section). All

the calculated Fano factors for all nuclides are given in the Supplementary Information 5.

As shown in Table 2, the Fano factors of GlassB are close to the ones (interquartiles ranges) of the NIST 612 glass and are lower than the Fano factors of the methods that require a pelletizing step.

The higher the Fano factor, the higher the difference with the Poisson's law, and so, the higher the contribution of other sources of errors to the global RSD. Considering that the NIST 612 and 614 glasses are homogenous, their Fano factors only depend on the variations of the flux of ablation particles, the ablation efficiency, the ionization efficiency,

Table 2 metadata of Fano factors for each analyzed material and sample preparation method

Grinding material	MixGlue		VanBind		SolGel		GlassB	NIST 612	NIST 614
	PTFE	WC	PTFE	WC	PTFE	WC	–	–	–
GS-N									
Average	747	448	1157	1427	885	440	27	162	109
Min	3	2	2	2	2	1	1	2	2
Quartile 1	19	6	15	16	16	5	2	18	4
Median	48	21	38	53	34	20	5	46	8
Quartile 3	352	104	364	565	288	144	18	159	17
Max	9703	6287	18,176	27,735	11,248	5719	231	2157	1354
NCS DC73301									
Average	650	208	607	691	323	162	13		
Min	2	1	2	2	2	1	1		
Quartile 1	28	9	21	21	16	7	2		
Median	62	30	53	77	48	20	4		
Quartile 3	544	126	450	451	257	127	10		
Max	11,693	3498	9783	8507	6177	2779	149		
ZW-C									
Average	979	814	744	607	694	289	135		
Min	2	2	2	2	2	2	2		
Quartile 1	21	19	19	15	16	9	3		
Median	87	61	85	84	42	36	6		
Quartile 3	432	327	455	360	262	168	21		
Max	18,670	13,262	10,167	8596	10,901	3650	3708		

the ion extraction and transmission efficiency. As stated before, the closeness between the Fano factors of GlassB and of the NIST glasses show that GlassB has homogeneity comparable to that of NIST 612 and 614. Methods that involve a pelletizing step have higher Fano factors compared to glasses, which is likely the consequence of a higher surface heterogeneity of the samples and a more unstable flux of ablation particles. Median Fano factors are lower when using PTFE material with the Sol–Gel and the MixGlue protocols, compared to the other pelletizing protocols. For the VandBind method, no significant distinctions could be made between the uses of the two grinding materials. Comparable results are obtained for the $\pm 3 \times SD$ filtration study and the examination of the RSD(int small).

Internal precision of signals measured for the internal standards

Homogeneity of the distribution of the internal standards within the sample is a crucial point. As they are not present within the grains, the internal standards should be homogeneously distributed between the grains and should not accumulate in some parts of the sample through a segregation process during the preparation step. Ideally, the internal precision of the measurements of the internal standards should be lower than or as close as possible to the ones of the analyzed elements with comparable counting statistics. Stability

of the signal obtained for Rh and In added to the studied materials as potential internal standards is compared with the ones of the other elements with a similar signal level. If the RSD(int small) obtained for In and Rh are similar (or even lower) than the ones of the nuclides of the CRMs for a similar signal intensity level, then the internal standards are regarded as well incorporated to the sample. The RSDs(int small) of In and Rh are gathered in the Table 3 for GS-N and in the Supplementary Information 6 for NCS DC73301 and ZW-C.

It appears that the RSDs(int small) obtained for Rh and In are close to the RSD(int small) of other signal-like nuclides for the four methods. In the case of GlassB, RSDs(int small) are relatively high because of the poor counting statistics. Therefore, in such cases, the internal standards can be regarded as well incorporated. The fact that the RSDs(int small) of the elements of the samples are overall higher than the ones of the internal standards for the methods which include a grinding step with PTFE balls could be explained by a lower dependence of In and Rh with respect to the CRMs granulometry. Although internal standards cannot be integrated inside the sample grains, they appear to be quite homogeneously distributed between the grains. In addition, the closeness between the RSDs(int small) of the internal standards and the ones of the most homogenous nuclides shows that no significant accumulation of internal standard occurs within the material (no “grains” of internal standard).

Table 3 intensities and RSD(int small) of the internal standards for the GS-N material and for the different sample preparation methods

Grinding material	MixGlue						VanBind						SolGel						GlassB						
	PTFE			WC			PTFE			WC			PTFE			WC			PTFE			WC			
	LR	MR	MR	LR	MR	MR	LR	MR	MR	LR	MR	MR	LR	MR	MR	LR	MR	MR	LR	MR	MR	LR	MR	MR	
¹⁰³ Rh	Concentration (ppm)	11.4			11.4			9.9			18.9			18.9			18.9			2.3			2.3		
	Intensity (counts)	2.1 × 10 ³	3.2 × 10 ²	2.2 × 10 ²	1.4 × 10 ³	2.2 × 10 ²	3.9 × 10 ³	5.2 × 10 ²	5.0 × 10 ³	5.0 × 10 ³	5.5 × 10 ²	4.9 × 10 ²	3.8 × 10 ³	4.9 × 10 ²	5.4 × 10 ³	9.3 × 10 ²	3.8 × 10 ³	4.9 × 10 ²	5.4 × 10 ³	1.0 × 10 ²	2.2 × 10 ¹	1.0 × 10 ²	2.2 × 10 ¹	2.2 × 10 ¹	
	RSD(int small)	23.1%	27.3%	20.9%	18.4%	20.6%	21.1%	20.6%	25.0%	25.0%	17.5%	25.3%	26.1%	25.3%	16.7%	13.6%	26.1%	25.3%	16.7%	22.0%	30.0%	22.0%	30.0%	30.0%	
	Sensitivity (counts/ppm)	1.8 × 10 ²	2.8 × 10 ¹	1.9 × 10 ¹	1.2 × 10 ²	5.3 × 10 ¹	4.0 × 10 ²	5.3 × 10 ¹	5.0 × 10 ²	5.0 × 10 ²	5.4 × 10 ¹	2.6 × 10 ¹	2.0 × 10 ²	2.6 × 10 ¹	2.8 × 10 ²	4.9 × 10 ¹	2.8 × 10 ²	2.6 × 10 ¹	2.8 × 10 ²	4.5 × 10 ¹	9.5 × 10 ⁰	4.5 × 10 ¹	9.5 × 10 ⁰		
¹¹⁵ In	Concentration (ppm)	11.4			11.4		9.9		10.1		10.1		18.9		18.9		18.9		18.9	2.3		2.3			
	Intensity (counts)	2.0 × 10 ³	2.7 × 10 ²	1.9 × 10 ²	1.4 × 10 ³	1.9 × 10 ²	5.9 × 10 ³	6.9 × 10 ²	6.4 × 10 ³	6.1 × 10 ²	6.1 × 10 ²	4.0 × 10 ³	4.0 × 10 ³	4.8 × 10 ²	5.5 × 10 ³	9.3 × 10 ²	4.0 × 10 ³	4.8 × 10 ²	5.5 × 10 ³	2.6 × 10 ²	5.0 × 10 ¹	2.6 × 10 ²	5.0 × 10 ¹		
	RSD(int small)	27.0%	33.4%	20.5%	18.3%	20.5%	18.4%	23.5%	25.0%	25.0%	21.5%	22.5%	22.5%	24.9%	16.1%	14.7%	22.5%	24.9%	16.1%	17.7%	23.5%	17.7%	23.5%		
	Sensitivity (counts/ppm)	1.7 × 10 ²	2.3 × 10 ¹	1.7 × 10 ¹	1.2 × 10 ²	7.0 × 10 ¹	6.0 × 10 ²	7.0 × 10 ¹	6.3 × 10 ²	6.1 × 10 ¹	6.1 × 10 ¹	2.5 × 10 ¹	2.1 × 10 ²	2.5 × 10 ¹	2.9 × 10 ²	4.9 × 10 ¹	2.9 × 10 ²	2.5 × 10 ¹	2.9 × 10 ²	1.1 × 10 ²	2.1 × 10 ¹	1.1 × 10 ²	2.1 × 10 ¹		

Thus, ¹¹⁵In and ¹⁰³Rh can be seen as possible candidates for internal standardization for quantitative analysis or imaging.

Results in Table 3 also show that sensitivity depends on the preparation method. The VanBind method allows higher sensitivity due to the absorption of the laser by the chromophore property of the binder, as demonstrated by O'Connor et al. [24].

Finally, the study of internal precision based on the signal stability (filtered values, RSD(int small) and Fano factors) revealed similar characteristics between NIST glasses and GlassB. Therefore, we conclude that these materials have similar levels of homogeneity. In comparison, the pellets present a more important heterogeneity (more unstable signals) which is the consequence of the persistence of a part of the initial granulometry in the pellets. Regarding the different methods which require a pelletizing, more stable signals are obtained when using WC as grinding material and for the MixGlue and SolGel preparation methods, which may indicate a better homogeneity than for the other pelletizing protocols.

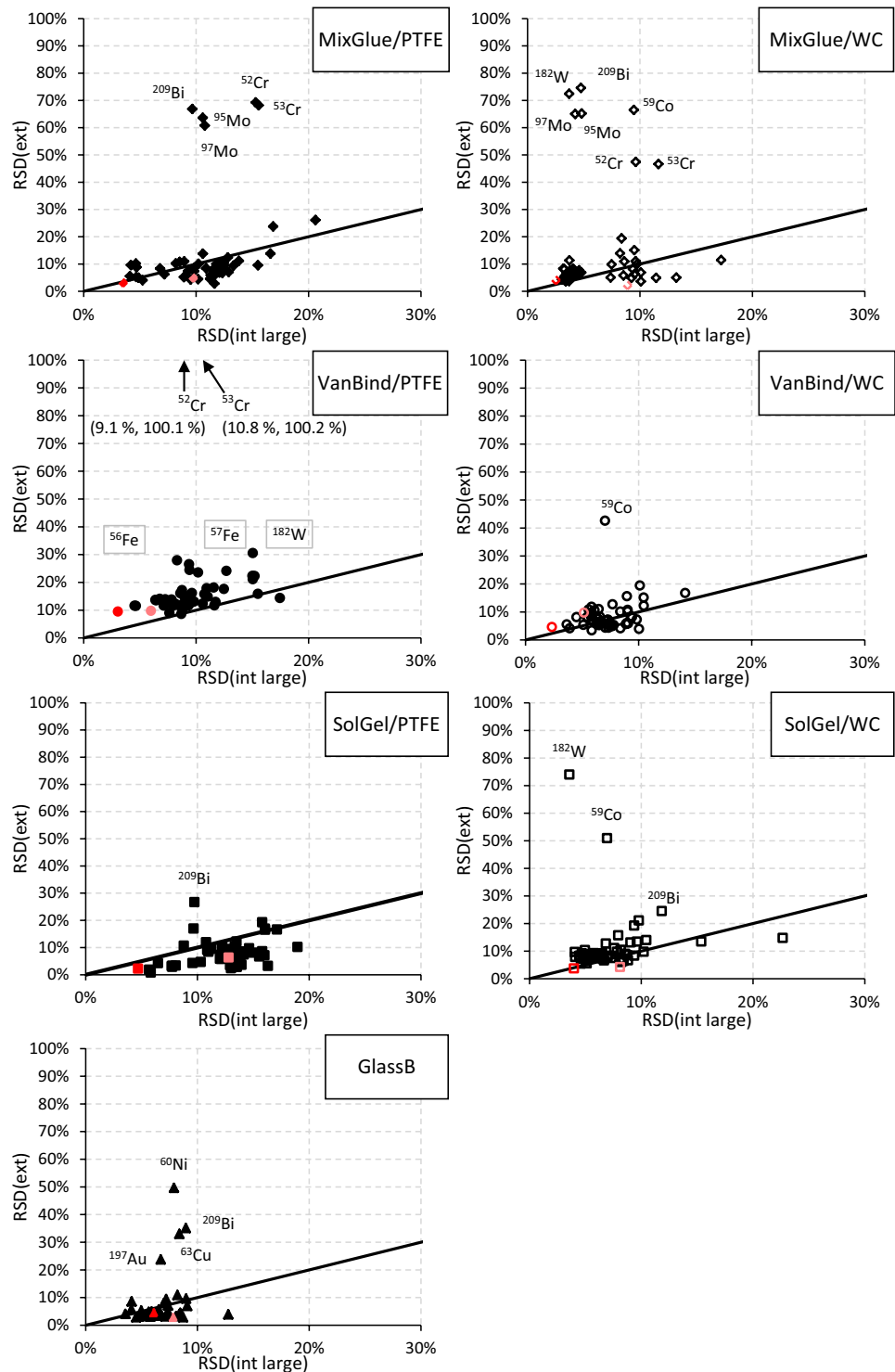
Reproducibility of the sample preparation methods (external precision)

Five replicates of the geostandard GS-N CRM were prepared to study the reproducibility of the method. The LA-ICP-MS analyzes were performed following the procedure described above.

In order to correct for sensitivity shift over time, signals of the nuclides of interest were normalized by the signal of ¹⁰³Rh used as an internal standard. So, average normalized intensity was calculated for each analyte in each replicate. Normalization was of importance here to correct for significant variations in the ICP-MS signal that occurred during the long time interval between two analyzes on the same sample (approximately 50 min). Then the obtained RSD(ext) was plotted as a function of the internal RSD(int large) for each nuclide and each preparation method (Fig. 5, Table 4 and detailed values in Supplementary Information 7). If RSD(ext) is lower than or close to the RSD(int large), then the inter-sample variability of the preparation method does not add significant variability to the elemental concentrations. In such cases, the method was considered as reproducible for the elements of interest for the analyzed geological materials.

RSDs(int large) are typically between 2–7% (minimal values) and 16–41% (maximal values) depending on the preparation methods. Variations of the RSD(ext) are even higher, between 1–9% and 27–100%, most likely as a result of contamination for some trace elements (see discussion below). Therefore, median RSD in the Table 4 are certainly a better indicator of reproducibility than average RSD, which may be strongly influenced by a few trace

Fig. 5 RSD(ext) plotted against RSD(int large) for all measured nuclides ($n = 3$) in the case of the GS-N geostandard material. The light red and dark red symbols are for In in the MR and the LR modes, respectively. The black line for all graphs is for RSD(int large) = RSD(ext). Outliers values for a few nuclides are identified in each graph



elements subject to contamination. Results show that median RSD(int large) and RSD(ext) are close for some preparation methods (MixGlue/WC, VanBind/PTFE, SolGel/WC, GlassB) whereas RSD(ext) are lower than RSD(int large) for the other methods (i.e., MixGlue/PTFE, VanBind/WC, SolGel/PTFE). This is consistent with visual examination of the graphs given in Fig. 5.

In addition, considering their first and third quartiles, RSD(int large) shows a more fluctuant signal for the pellets after PTFE grinding (9.8–15.4% for MixGlue and 17.1–22.2% for SolGel), compared to the pellets after grinding with WC balls (9.9–12.8% for MixGlue and 9.8–11.9% for SolGel) and the GlassB method (12.0–14.3%).

Table 4 metadata of the RSD(int large) and the RSD(ext) measured for GS-N material in the LR and MR modes for the different preparation methods

	MixGlue				VanBind				SolGel				GlassB			
	PTFE		WC		PTFE		WC		PTFE		WC		PTFE		WC	
	RSD(int large)	RSD(ext)	RSD(int large)	RSD(ext)	RSD(int large)	RSD(ext)	RSD(int large)	RSD(ext)	RSD(int large)	RSD(ext)	RSD(int large)	RSD(ext)	RSD(int large)	RSD(ext)	RSD(int large)	RSD(ext)
Average	11.8	14.1	8.4	14.6	14.5	18.6	9.6	9.6	8.7	16.3	8.0	10.5	11.5	7.8	7.8	7.8
Standard deviation	3.7	17.5	3.2	19.5	4.8	17.0	3.2	3.2	5.9	4.4	5.0	5.0	11.0	4.4	4.4	9.8
Min	5.1	2.9	4.3	2.2	4.1	8.7	2.4	2.4	3.5	6.5	0.8	5.5	3.8	3.1	3.1	2.9
Quartile 1	9.8	5.9	6.1	5.7	11.1	12.4	8.2	8.2	5.4	14.0	4.1	7.9	7.6	3.8	3.8	3.5
Median	12.2	8.6	7.5	6.8	14.0	13.7	9.0	9.0	7.3	16.4	7.4	9.9	8.5	6.2	6.2	4.3
Quartile 3	14.5	10.6	10.7	11.0	17.2	17.7	10.7	10.7	10.2	18.6	9.6	11.2	10.4	12.6	12.6	7.0
Max	21.1	69.3	16.1	74.6	27.8	100.2	21.6	21.6	42.7	27.0	26.7	41.0	74.0	15.9	15.9	49.7

RSD are given in percentages. Average values ($n=5$) are those of all the nuclides

Therefore, we can conclude that the studied methods are reproducible for the majority of the analyzed nuclides, including In. However, there are exceptions for some methods.

First, the use of WC grinding material cause contamination in W and Co. The manufacturer of the WC material mentioned these contamination risks. An Au contamination is noticed for GlassB. The source of this contamination is the crucibles used for the fusion, as they contain 5% of Au.

Cr and Fe contamination are observed for some of the methods, including a pelletizing step. Actually, Fe and Cr particles have been observed on the pellet surfaces by SEM-EDS for each pelletizing protocol (Supplementary Information 8). These particles likely come from the disks of the press, which are made of a Fe-Cr alloy. By the way, none of these Fe-Cr particles were observed in the GS-N CRM before its preparation. The contamination in such particles is higher in the case of the mixing with glue because the material is firmly stuck to the metallic disks of the press mold and, therefore, may snatch more particles from the disks; conversely, the SolGel is the most friable and less sticky mixture and presents lower contamination risks. It should be mentioned that the random presence of Fe-Cr particles only affects inter-preparation reproducibility in the case of Cr. Actually, due to the high proportion of Fe in the GS-N CRM ($\approx 39\ 000$ ppm) the signal from the particles from the mold is nonsignificant with respect to the signal which came from the geological material. To go further in the investigations, a square surface was ablated ($\approx 1\ \text{mm}^2$) and no Fe-Cr particles have been found in the ablation crater by SEM-EDS observation, which supports the hypothesis that this contamination is only on the pellet surfaces. Therefore, a pre-ablation path could avoid bias on the results. However, in a perspective of industrialization of the process, it is important to reduce the processing time. As a pre-ablation step would significantly increase the analysis time, this option was not considered in this study.

Last, inter-preparation measurements are not reproducible for a few elements and sample preparation methods: Cu for GlassB, Mo and Bi for MixGlue (regardless of the composition of the grinding balls) and Ni for GlassB and SolGel/WC. No explanations were found except random contaminations in these elements in the course of the preparation process. Cu and Mo are ubiquitous elements and can be observed in airborne particles in laboratory atmospheres. Mo and Bi are present only at trace levels in the GS-N CRM (1.2 and 0.18 ppm respectively against 20 ppm for Cu and 34 ppm for Ni) and are therefore vulnerable to contamination.

Physical considerations about the samples

First, a common drawback of the pelletizing methods is the persistence of the largest mineral grain in the mixture, which limits homogeneity of the samples. Indeed, some large mineral grains remaining on the pellet surface and were observed with the laser camera. Pellets have the advantage to have a higher sample proportion in the final preparation (77% for MixGlue, 60% for VanBind and 55% for SolGel) in contrast with the glass beads (8.5%). The low proportion of binders and reagents allow the reduction of the contamination risks by these chemical products. In addition, no high heating step is necessary to obtain the pellets ($T \leq 110$ °C) in contrast with the GlassB method (1055 °C) which conduce to the evaporation of volatile elements (As, Se, Cd, Zn and Te whose boiling temperatures are 616 °C, 685 °C, 767 °C, 907 °C and 988 °C respectively).

Advantages of the use of the vanillic acid as an organic binder were previously mentioned by O'Connor et al. [24] for analyzes with a 213 nm ablation laser system. Firstly, an improvement of the sensitivity due to a great absorption of the laser energy than other binders, as observed in this work. Secondly, the great absorption of the 213-nm laser energy also allows the formation of smaller ablation particles and thus reduces elemental fractionation compared to other binders.

The advantages of the SolGel method are the formation of a matrix chemically close to that of NIST glasses (SiO_2) without any high temperature heating step contrary to alkaline fusion. However, a drawback is that the pellets are not as mechanically robust as the ones prepared by means of the other methods.

Finally, the alkaline fusion to prepare glass beads has several advantages as follows: (1) the formation of a matrix close to that of NIST glasses which could be used as standards for quantitative analyzes (glassy sample), (2) suppression of mineralogical differentiation and grain effects, (3) a longer conservation time (notably fewer risks of degradation by adsorption of water than for the pellets). In addition, it is not possible to quantify Li and B with the protocol used.

Conclusions

Four sample preparation methods were compared for LA-ICP-MS analyzes. This comparison shows that signals are less stable for the preparation methods that involve a pelletizing step, especially when the grinding step was performed with PTFE balls, with respect to glass beads prepared by alkaline fusion and NIST glass reference materials. The difference was strongly reduced when the grinding was performed with WC instead of PTFE, but only in the case of the MixGlue and SolGel methods. RSDs(int large) were

also improved when using WC grinding material, except for the VanBind method.

Signal fluctuations of the GlassB samples were comparable to the ones of the NIST glasses. Therefore, the GlassB samples may be regarded as homogeneous at the scale of the analyzed volumes by LA-ICP-MS. The poorer internal precisions observed for pellets may be due to the persistence of the "grain effect", i.e., the largest mineral grains in the pellet samples, even when grinding is carried out with WC balls. However, considering the pelletizing methods, the signal stability was improved for the SolGel and the MixGlue process when using WC material to grind the sample.

In addition, small-scale RSD no longer decreased for number counts above 10^3 counts, as statistical error becomes negligible with respect to other sources of errors, here mainly due to the variations of the ablation efficiency and the homogeneity of the sample. Therefore, best RSD(int small) were typically 14% for GlassB, 18% for SolGel/WC and 21% for MixGlue/WC, with the selected acquisition parameters. So, the GlassB method should be preferred regarding internal repeatability (14%). To compare specifically the pelletizing methods, VanBind led to less homogeneous samples than MixGlue and SolGel. Besides, the use of WC material improves the signal stability for MixGlue and SolGel methods, but has no influence in the case of the VanBind method.

Addition of liquid internal standards for all of the preparation methods was regarded as efficient as RSD(int small) of these elements are close to (GlassB and grinding with WC balls) or even lower (grinding with PTFE balls) than those of most of the analyzed elements with comparable signal intensity.

Lastly, the four preparation methods were reproducible for the majority of the 59 analyzed nuclides. Lack of reproducibility was observed for some specific elements and for some specific methods (Cr, Fe, Co, Ni, Cu, Mo, W, Au and Bi) mainly because of variable contamination by materials used in the preparation process. Therefore, as a significant part of the final uncertainty budget was due to the sample heterogeneity, the preparation method must be chosen according to the requested uncertainties and the targeted elements.

A future work is the realization of quantitative analyzes to compare the accuracy, the precision, and the detection limits obtained with the four preparation methods applied to the same samples.

Supplementary Information The online version contains supplementary material available at <https://doi.org/10.1007/s44211-023-00309-5>.

Acknowledgements This work was performed with financial backing of a PhD thesis from Orano Mining and the CEA/DAM/DIF. The authors would like to express their gratitude to Valérie Granger, Mike Maury and Magali Celier (Orano Mining, CIME) for the main lines of

the alkaline fusion protocol, the formation on the Katanax X-Fluxer X-600 and of their reception during the preparation of the glass beads. Authors would thank Olivier Marie (CEA, DAM/DIF) for the MEB imaging. Authors would also thank Aurélie Diacre (CEA, DAM/DIF and LSCE) for the laser granulometry measurements. Finally, authors express their gratitude to the two anonymous reviewers for their time and their helpful comments.

Author contributions MS: writing—original draft, data curation, formal analysis, software, investigation. AL–G: data curation, formal analysis, investigation. A–CH: methodology, writing review and editing, supervision. FP: methodology, writing review and editing, supervision. CP: methodology, writing review and editing, supervision.

Data availability The data presented in this study are available on request from the corresponding author.

Declarations

Conflict of interest There are no competing interests to declare.

References

1. F. Nehring, D.E. Jacob, M.G. Barth, S.F. Foley, Laser-ablation ICP-MS analysis of siliceous rock glasses fused on an iridium strip heater using MgO dilution. *Microchim Acta* **160**(1–2), 153–163 (2008). <https://doi.org/10.1007/s00604-007-0819-7>
2. J.S. Fedorowich, J.P. Richards, J.C. Jain, R. Kerrich, J. Fan, A rapid method for REE and trace-element analysis using laser sampling ICP-MS on direct fusion whole-rock glasses. *Chem. Geol.* **106**(3–4), 229–249 (1993). [https://doi.org/10.1016/0009-2541\(93\)90029-1](https://doi.org/10.1016/0009-2541(93)90029-1)
3. M. Petrelli, D. Perugini, G. Poli, A. Peccerillo, Graphite electrode lithium tetraborate fusion for trace element determination in bulk geological samples by laser ablation ICP-MS. *Microchim Acta* **158**(3–4), 275–282 (2007). <https://doi.org/10.1007/s00604-006-0731-6>
4. V. Kanicky, J.-M. Mermet, Use of a single calibration graph for the determination of major elements in geological materials by laser ablation inductively coupled plasma atomic emission spectrometry with added internal standards. *Fr. J. Anal. Chem.* **363**(3), 294–299 (1999). <https://doi.org/10.1007/s002160051191>
5. S.A. Baker, M. Bi, R.Q. Aucelio, B.W. Smith, J.D. Winefordner, Analysis of soil and sediment samples by laser ablation inductively coupled plasma mass spectrometry. *J. Anal. At. Spectrom.* **14**(1), 19–26 (1999). <https://doi.org/10.1039/a804060e>
6. D. Günther, A.V. Quadt, R. Wirz, H. Cousin, V.J. Dietrich, Elemental analyses using laser ablation-inductively coupled plasma-mass spectrometry (LA-ICP-MS) of geological samples fused with Li 2 B 4 O 7 and calibrated without matrix-matched standards. *Microchim. Acta* **136**(3–4), 101–107 (2001). <https://doi.org/10.1007/s006040170038>
7. I. Hubová, M. Holá, J. Pinkas, V. Kanický, Examination of sol–gel technique applicability for preparation of pellets for soil analysis by laser ablation inductively coupled plasma optical emission spectrometry. *J. Anal. At. Spectrom.* **22**(10), 1238–1243 (2007). <https://doi.org/10.1039/b701555k>
8. B. Fernández, F. Claverie, C. Pécheyan, O.F.X. Donard, Solid-spiking isotope dilution laser ablation ICP-MS for the direct and simultaneous determination of trace elements in soils and sediments. *J. Anal. At. Spectrom.* **23**(3), 367–377 (2008). <https://doi.org/10.1039/B711247E>
9. K. Ito et al., LA-ICP-MS analysis of pressed powder pellets to luminescence geochronology. *Chem. Geol.* **262**(3–4), 131–137 (2009). <https://doi.org/10.1016/j.chemgeo.2009.01.003>
10. L. Arroyo, T. Trejos, P.R. Gardinali, J.R. Almirall, Optimization and validation of a laser ablation inductively coupled plasma mass spectrometry method for the routine analysis of soils and sediments. *Spectrochim. Acta Part B At. Spectrosc.* **64**(1), 16–25 (2009). <https://doi.org/10.1016/j.sab.2008.10.027>
11. K.P. Jochum et al., Accurate trace element analysis of speleothems and biogenic calcium carbonates by LA-ICP-MS. *Chem. Geol.* **318–319**, 31–44 (2012). <https://doi.org/10.1016/j.chemgeo.2012.05.009>
12. J. Malherbe, F. Claverie, A. Alvarez, B. Fernandez, R. Pereira, J.L. Molloy, Elemental analyses of soil and sediment fused with lithium borate using isotope dilution laser ablation-inductively coupled plasma-mass spectrometry. *Anal. Chim. Acta* **793**, 72–78 (2013). <https://doi.org/10.1016/j.aca.2013.07.031>
13. M.S. de la Torre et al., Applying ED-XRF and LA-ICP-MS to geochemically characterize chert. The case of the Central-Eastern Pre-Pyrenean lacustrine cherts and their presence in the Magdalenian of NE Iberia. *J. Archaeol. Sci. Rep.* **13**, 88–98 (2017). <https://doi.org/10.1016/j.jasrep.2017.03.037>
14. V.M. Neves, G.M. Heidrich, F.B. Hanzel, E.I. Muller, V.L. Dressler, Rare earth elements profile in a cultivated and non-cultivated soil determined by laser ablation-inductively coupled plasma mass spectrometry. *Chemosphere* **198**, 409–416 (2018). <https://doi.org/10.1016/j.chemosphere.2018.01.165>
15. A.M. Horne, M.C. van Soest, K.V. Hodges, A. Tripathy-Lang, J.K. Hourigan, Integrated single crystal laser ablation U/Pb and (U–Th)/He dating of detrital accessory minerals – proof-of-concept studies of titanites and zircons from the Fish Canyon tuff. *Geochim. Cosmochim. Acta* **178**, 106–123 (2016). <https://doi.org/10.1016/j.gca.2015.11.044>
16. T.L. Spano, A. Simonetti, E. Balboni, C. Dorais, P.C. Burns, Trace element and U isotope analysis of uraninite and ore concentrate: Applications for nuclear forensic investigations. *Appl. Geochem.* **84**, 277–285 (2017). <https://doi.org/10.1016/j.apgeochem.2017.07.003>
17. S.V. Jovanovic, T. Kell, J. El-Haddad, C. Cochrane, C. Drummond, A. El-Jaby, Trace analysis of uranium ore concentrates using laser ablation inductively coupled plasma mass spectrometry for nuclear forensics. *J. Radioanal. Nucl. Chem.* (2020). <https://doi.org/10.1007/s10967-019-06991-y>
18. P. Lach, J. Mercadier, J. Dubessy, M.-C. Boiron, M. Cuney, In situ quantitative measurement of rare earth elements in uranium oxides by laser ablation-inductively coupled plasma-mass spectrometry. *Geostand. Geoanal. Res.* (2013). <https://doi.org/10.1111/j.1751-908X.2012.00161.x>
19. W.D. Stoner, The analytical nexus of ceramic paste composition studies: A comparison of NAA, LA-ICP-MS, and petrography in the prehispanic Basin of Mexico. *J. Archaeol. Sci.* **76**, 31–47 (2016). <https://doi.org/10.1016/j.jas.2016.10.006>
20. B. Siqin, Q.-H. Li, F.-X. Gan, Analysis of some chinese potash glass by laser ablation-inductively coupled plasma-atomic emission spectrometry and laser ablation-inductively coupled plasma-mass spectrometry. *Chin. J. Anal. Chem.* (2013). [https://doi.org/10.1016/S1872-2040\(13\)60678-7](https://doi.org/10.1016/S1872-2040(13)60678-7)
21. S.M. Eggins, Laser ablation ICP-MS analysis of geological materials prepared as lithium borate glasses. *Geostand. Geoanal. Res.* (2003). <https://doi.org/10.1111/j.1751-908X.2003.tb00642.x>
22. G. Bauer, A. Limbeck, Quantitative analysis of trace elements in environmental powders with laser ablation inductively coupled mass spectrometry using non-sample-corresponding reference materials for signal evaluation. *Spectrochim. Acta Part B At. Spectrosc.* **113**, 63–69 (2015). <https://doi.org/10.1016/j.sab.2015.09.007>
23. A.L. Gray, Solid sample introduction by laser ablation for inductively coupled plasma source mass spectrometry. *Analyst* (1985). <https://doi.org/10.1039/an9851000551>

24. C. O'Connor, M.R. Landon, B.L. Sharp, Absorption coefficient modified pressed powders for calibration of laser ablation inductively coupled plasma mass spectrometry. *J. Anal. At. Spectrom.* **22**(3), 273–282 (2007). <https://doi.org/10.1039/B612512C>
25. G. Steinhöfel, J. Breuer, F. von Blanckenburg, I. Horn, D. Kaczorek, M. Sommer, Micrometer silicon isotope diagnostics of soils by UV femtosecond laser ablation. *Chem. Geol.* (2011). <https://doi.org/10.1016/j.chemgeo.2011.05.013>
26. I. Hubová, M. Holá, J. Pinkas, V. Kanický, Examination of sol–gel technique applicability for preparation of pellets for soil analysis by laser ablation inductively coupled plasma optical emission spectrometry. *J. Anal. At. Spectrom.* (2007). <https://doi.org/10.1039/b701555k>
27. A.J. Fitzpatrick, T. Kurtis Kyser, D. Chipley, D. Beauchemin, Fabrication of solid calibration standards by a sol–gel process and use in laser ablation ICPMS. *J. Anal. At. Spectrom.* (2008). <https://doi.org/10.1039/B712366C>
28. W.C. Davis, S.J. Christopher, G.C. Turk, Simultaneous mass bias and fractionation corrections utilizing isotopic solid standards and laser ablation ICPMS. *Anal. Chem.* (2005). <https://doi.org/10.1021/ac050872p>
29. W. Klemm, G. Bombach, A simple method of target preparation for the bulk analysis of powder samples by laser ablation inductively coupled plasma mass spectrometry (LA-ICP-MS). *Fr. J. Anal. Chem.* (2001). <https://doi.org/10.1007/s002160100848>
30. D. Garbe-Schönberg, S. Müller, Nano-particulate pressed powder tablets for LA-ICP-MS. *J. Anal. At. Spectrom.* **29**(6), 990–1000 (2014). <https://doi.org/10.1039/C4JA00007B>
31. K.P. Jochum et al., Nano-powdered calcium carbonate reference materials: significant progress for microanalysis? *Geostand. Geoanal. Res.* **43**(4), 595–609 (2019). <https://doi.org/10.1111/ggr.12292>
32. S.C. Jantzi, J.R. Almirall, Elemental analysis of soils using laser ablation inductively coupled plasma mass spectrometry (LA-ICP-MS) and laser-induced breakdown spectroscopy (LIBS) with multivariate discrimination: tape mounting as an alternative to pellets for small forensic transfer specimens. *Appl Spectrosc* (2014). <https://doi.org/10.1366/13-07351>
33. L.P. Bédard, D.R. Baker, N. Machado, A new technique for the synthesis of geochemical reference samples for laser ablation-ICP-MS analysis of zircons. *Chem. Geol.* (1997). [https://doi.org/10.1016/S0009-2541\(96\)00169-6](https://doi.org/10.1016/S0009-2541(96)00169-6)
34. M. Pakieła, M. Wojciechowski, B. Wagner, E. Bulska, A novel procedure of powdered samples immobilization and multi-point calibration of LA ICP MS. *J. Anal. At. Spectrom.* (2011). <https://doi.org/10.1039/c0ja00201a>
35. W. Zhang et al., Quantitative analysis of major and trace elements in NH₄HF₂-modified silicate rock powders by laser ablation - inductively coupled plasma mass spectrometry. *Anal. Chim. Acta* **983**, 149–159 (2017). <https://doi.org/10.1016/j.aca.2017.06.039>
36. S. Wu, V. Karius, B.C. Schmidt, K. Simon, G. Wörner, Comparison of ultrafine powder pellet and flux-free fusion glass for bulk analysis of granitoids by laser ablation-inductively coupled plasma-mass spectrometry. *Geostand. Geoanal. Res.* (2018). <https://doi.org/10.1111/ggr.12230>
37. C. Simons et al., Comparative study on the homogeneity of polymeric calibration materials using LA-ICP-MS. *J. Anal. At. Spectrom.* **23**(7), 1038 (2008). <https://doi.org/10.1039/b719145f>
38. M. Thompson, J.E. Goulter, F. Sieper, Laser ablation for the introduction of solid samples into an inductively coupled plasma for atomic-emission spectrometry. *Analyst* **106**(1258), 32 (1981). <https://doi.org/10.1039/an9810600032>
39. S.E. Gilbert et al., Optimisation of laser parameters for the analysis of sulphur isotopes in sulphide minerals by laser ablation ICP-MS. *J. Anal. At. Spectrom.* **29**(6), 1042–1051 (2014). <https://doi.org/10.1039/C4JA00011K>
40. D.G. Reading, I.W. Croudace, P.E. Warwick, Fusion bead procedure for nuclear forensics employing synthetic enstatite to dissolve uraniferous and other challenging materials prior to laser ablation inductively coupled plasma mass spectrometry. *Anal. Chem.* (2017). <https://doi.org/10.1021/acs.analchem.7b00558>
41. D. Peters, T. Pettke, Evaluation of major to ultra trace element bulk rock chemical analysis of nanoparticulate pressed powder pellets by LA-ICP-MS. *Geostand. Geoanal. Res.* **41**(1), 5–28 (2017). <https://doi.org/10.1111/ggr.12125>
42. R. Hinton, B. Harte, G. Witt-Eickschen, Ion probe measurements of national institute of standards and technology standard reference material SRM 610 glass, trace elements. *Analyst* **120**, 1315–1319 (1995)
43. J. Kane, A history of the development and certification of NIST glass SRMs 610–617. *Geostand. Newsl. J. Geostand. Geoanal.* **22**(1), 7–13 (1998)
44. M. Motelica-Heino, S. Rauch, G.M. Morrison, O.F.X. Donard, Determination of palladium, platinum and rhodium concentrations in urban road sediments by laser ablation-ICP-MS. *Anal. Chim. Acta* **436**(2), 233–244 (2001). [https://doi.org/10.1016/S0003-2670\(01\)00967-9](https://doi.org/10.1016/S0003-2670(01)00967-9)
45. R.E. Russo, X.L. Mao, C. Liu, J. Gonzalez, Laser assisted plasma spectrochemistry: laser ablation. *J. Anal. At. Spectrom.* (2004). <https://doi.org/10.1039/b403368j>
46. J. González, C. Liu, X. Mao, R.E. Russo, UV-femtosecond laser ablation-ICP-MS for analysis of alloy samples. *J. Anal. At. Spectrom.* **19**(9), 1165–1168 (2004). <https://doi.org/10.1039/B403205E>
47. M. Neuilly, Modelling and estimation of measurement errors. *Meas. Sci. Technol.* **11**, 1825 (2000). <https://doi.org/10.1088/0957-0233/11/12/701>
48. U. Fano, Ionization yield of radiations. II. The fluctuations of the number of ions. *Phys. Rev.* **72**(1), 1 (1947). <https://doi.org/10.1103/PhysRev.72.26>
49. V. Bora et al., Estimation of Fano factor in inorganic scintillators from time correlations. in *2015 IEEE Nuclear Science Symposium and Medical Imaging Conference (NSS/MIC)* (San Diego, CA, USA, 2015), pp. 1–3. <https://doi.org/10.1109/NSSMIC.2015.7581943>
50. M. Guillon, I. Horn, D. Günther, A comparison of 266 nm, 213 nm and 193 nm produced from a single solid state Nd:YAG laser for laser ablation ICP-MS. *J. Anal. At. Spectrom.* **18**(10), 10 (2003). <https://doi.org/10.1039/B305434A>

Springer Nature or its licensor (e.g. a society or other partner) holds exclusive rights to this article under a publishing agreement with the author(s) or other rightsholder(s); author self-archiving of the accepted manuscript version of this article is solely governed by the terms of such publishing agreement and applicable law.